Journal of Solid State Chemistry 181 (2008) 2899–2907

Contents lists available at ScienceDirect

Journal of Solid State Chemistry

journal homepage: www.elsevier.com/locate/jssc

Porous framework of $T_2[Fe(CN)_6]\cdot xH_2O$ with T = Co, Ni, Cu, Zn, and H_2 storage

M. Avila [a], L. Reguera [b], J. Rodríguez-Hernández [c], J. Balmaseda [d], E. Reguera [a,c,*]

[a] Centro de Investigación en Ciencia Aplicada y Tecnología Avanzada-Unidad Legaria, IPN, México, D.F.
[b] Facultad de Química, Universidad de La Habana, Cuba
[c] Instituto de Ciencia y Tecnología de Materiales, Universidad de La Habana, Cuba
[d] Departamento de Polímeros, Instituto de Investigaciones en Materiales, Universidad Nacional Autónoma de México, México, D.F., México

ARTICLE INFO

Article history:
Received 23 May 2008
Accepted 20 July 2008
Available online 30 July 2008

Keywords:
Crystal chemistry
Prussian blue
Hydrogen storage
Structural studies

ABSTRACT

The materials under study were prepared from aqueous solutions of ferrocyanic acid and salts of the involved transition metals and their crystal structure solved and refined from X-ray powder diffraction data. Complementary information from thermogravimetric, infrared and Mössbauer data was also used for the structural study. Three different crystal structures were found: hexagonal (P-3) for Zn with the zinc atom coordinated to three N ends of CN groups plus a water molecule, cubic (Pm-3m) for Ni and Cu, and monoclinic ($P2_1/m$) for Co. For Ni and Cu the obtained solids have an open channel framework related to 50% of vacancies for the building unit, $[Fe(CN)_6]$. In the as-synthesized material the framework free volume is occupied by coordinated and hydrogen-bonded water molecules. These of hexacyanoferrates (II) have received certain attention as prototype of materials for the hydrogen storage. In the anhydrous phase of Ni and Cu, 50% of the metal (T) coordination sites, located at the cavities surface, will be available to interact with the hydrogen molecule. However, when the crystal waters are removed the porous frameworks collapse as it is suggested by H_2 and CO_2 adsorption data. For Co, a structure of stacked layers was found where the cobalt atoms have both tetrahedral and octahedral coordination. The layers remain together through a network of hydrogen-bonding interactions between coordinated and weakly bonded water molecules. No H_2 adsorption was observed in the anhydrous phase of Co. For Zn, the porous framework remains stable on the water removal but with a system of narrow channels and a small available volume, also inaccessible to H_2.

1. Introduction

Transition metal hexacyanometallates have received relatively large attention in the last few years. This family of coordination polymers has been studied as prototype of molecular magnets [1–5] and more recently as materials for the hydrogen storage [6–12]. The CN ligand has the ability to serve as bridge group between neighboring metal centers, removing electron density from the metal linked at its C end, through a π back-bonding interaction, to increase the charge density on the N end that is the coordination site for the other metal. This leads to the overlapping between the electron clouds of neighboring metal centers and to their spin coupling and, thereby, a magnetic ordering is established. This supports the role of hexacyanometallates as prototype of molecular magnets. The same mechanism explains the relatively large ability that some porous hexacyanometallates show for the hydrogen storage [12]. The electron density concentration at the N end contributes to increase the electric field gradient at the cavity surface, enhancing the framework interaction with the quadrupole moment of the hydrogen molecule. This interaction allows the H_2 stabilization within the cavity. In addition, the anhydrous phase of porous hexacyanometallates with cubic structure has metal centers with open coordination sphere at the cavity surface. The possibility of H_2 coordination to these metal sites has also motivated the interest of hexacyanometallates as prototype of porous solids for the hydrogen storage.

The best-known hexacyanometallates are the so-called Prussian blue (PB) analogues, where the involved transition metals have octahedral coordination and in the –M–C–N–T–N–C–M– sequence [13]. This series of compounds crystallizes with a cubic or pseudo-cubic unit cell, usually in the highly symmetric Fm-3m space group [13]. Deviations or atypical structures regarding PB analogues are known. In hexacyanometallates (II) and some hexacyanometallates (III) the Zn atom is found with tetrahedral

* Corresponding author at: Instituto de Ciencia y Tecnologia de Materiales, Universidad de La Habana, La Ciudad de La Habana, Cuba. Fax: +53 7 29 6000.
E-mail address: ereguera@yahoo.com (E. Reguera).

0022-4596/$ - see front matter © 2008 Elsevier Inc. All rights reserved.
doi:10.1016/j.jssc.2008.07.030

coordination [14]; for Mn and Cd hexacyanometallates (II) a different metals sequence is observed, –M–C–N–*T*…*T*–N–C–M– [15,16], and there are compositions where the N end behaves as a bifurcated ligand coordinating two *T* metals [17]. Within the series $T_2[Fe(CN)_6]\cdot xH_2O$ with T = Mn, Co, Ni, Cu, Zn, Cd; only for Mn and Cd the crystal structure is known [15,16]. For Co, Ni, Cu, and Zn the structure and related properties remain unknown. In this contribution the crystal structures and properties for these four metals are reported, where atypical structures for Co and Zn were also observed. This series of hexacyanoferrates (II) has attracted certain attention as prototype of materials for the hydrogen storage [9], supposing that it has a PB analogues type structure with 50% of vacancy for the building unit, $[Fe(CN)_6]$, and as a consequence, with also 50% of available metal (T) coordination sites at the cavities surface to interact with hydrogen molecule once the crystal water is removed. This supposes that the framework is preserved for the anhydrous phase. Our results, based on a detailed structural study, herein discussed, are quite different. For Ni and Cu on the water removal the porous framework collapses. For Co, a structure of stacked layers was observed. Neighboring layers remain linked through a network of hydrogen-bonding interactions between coordinated and weakly bonded waters. For Zn, the porous framework remains stable but with a system of narrow channels and a small free volume.

2. Experimental section

The samples to be studied were obtained by mixing aqueous solutions (0.01 M) of the metal chloride (in excess) and ferrocyanic acid ($H_4[Fe(CN)_6]$ prepared *in situ* [18]). The precipitate formed was aged 24 h within the mother liquor, then separated by filtration and washed several times with distilled water and finally air dried until it had a constant weight. The same result was obtained from metal sulfate or nitrate. When these compounds are precipitated from sodium or potassium ferrocyanides, the mixed salts containing Na or K are obtained. The nature of the obtained solids was established from energy-dispersed spectroscopy (EDS) analyses, X-ray diffraction (XRD), and infrared (IR) and Mössbauer data. The degree of hydration and thermal stability of the samples were estimated by using thermogravimetric (TG) curves. The metal atomic ratio found from EDS spectra for the obtained solids, close to 2:1, agrees with the expected formula unit, $T_2[Fe(CN)_6]\cdot xH_2O$.

The TG curves were run under an N_2 atmosphere (100 ml min^{-1}) using a thermo-balance (TGA 2950 model from TA instruments) operated in the high-resolution mode. IR spectra were collected by the KBr pressed disk technique using an FT spectrophotometer (Spectrum One from Perkin Elmer). The Mössbauer spectra were recorded at room temperature with a constant acceleration spectrometer operated in the transmission mode and a ^{57}Co/Rh source. The spectra were fitted by a least-squares minimization algorithm and pseudo-Lorentzian line shape in order to obtain the values for isomer shift (δ), quadrupole splitting (Δ) and linewidth (Γ). The value of δ is reported relative to sodium nitroprusside. The XRD powder patterns were recorded in the Bragg–Brentano geometry using Cu$K\alpha$ radiation and an HZG4 diffractometer. All the patterns were collected from 5° to 90°/2θ with a step size of 0.025°. The XRD powder patterns were indexed using DICVOL program [19]. The crystal structures were solved *ab initio* by direct methods using the program SHELXS [20] from extracted intensities according to the Le Bail method [21]. Physical considerations and information from the remaining techniques were used in order to select the appropriate structural models to be refined, and then to check the obtained structure. The structure refinement was then carried out in parallel for all the probable space groups. The structural refinement was performed with the Rietveld method using the FullProf program [22] and the pseudo-Voigt peak shape function. Peak profiles were calculated within 10 times the full width at half maximum (FWHM). The background was modeled by a third-order polynomial.

The CO_2 and H_2 adsorption isotherms were recorded using ASAP 2010 and 2020 analyzers (from Micromeritics), respectively. Sample tubes of known weight were loaded with 40–50 mg of sample and sealed using TranSeal. Previous to CO_2 and H_2 adsorption, the samples were degassed on the ASAP analyzer using a heating rate of 1 °C/min and then maintained at the dehydration temperature indicated by the TG curve to obtain a stable outgas rate below 1-μm Hg. The degassed sample and sample tube were weighed and then transferred back to the analyzer with the TranSeal preventing exposure of the sample to air. After volume measurement with He the degassing was continued for 24 h at the dehydration temperature in the sample port. Measurements were performed at 273 K for CO_2 using an ice-water bath and at 75 K for H_2 using a liquid N_2 bath.

3. Results and discussion

3.1. Hydration degree and thermal stability

Fig. 1 shows the TG curves for the studied series of hexacyanoferrates (II). The smallest hydration degree and the higher thermal stability were observed for Zn. According to the weight loss this compound crystallizes with about 2.3 water molecules per formula unit. Below 50 °C approximately 0.3 water molecules per formula evolves, probably weakly bonded waters. This small amount of weakly bonded waters suggests that this compound has a compact structure. The cavities of porous hexacyanometallates are usually occupied by hydrogen-bonded water molecules [23]. Then, from 160 °C the remaining two water molecules abandon the solid together to form an anhydrous phase that remains stable up to above 350 °C. The relatively high temperature which these two water molecules evolve suggests that they are coordinated. This corresponds to a coordinated water molecule per Zn atom. According to the formula unit there are six

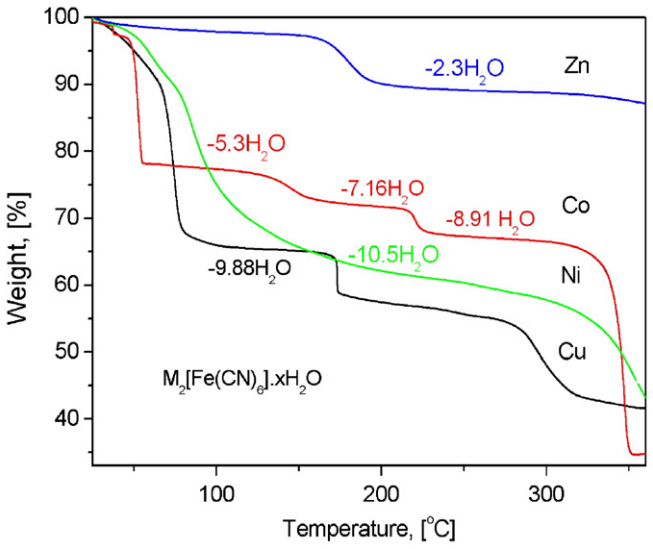

Fig. 1. TG curves for the studied series of divalent transition metal hexacyanoferrates (II).

N ends available for the two Zn atoms coordination. This suggests that the coordination environment for the Zn atom is probably formed by three N ends plus a water molecule, in a pseudo-tetrahedral configuration.

For Ni and Cu a relatively large amount of water molecules evolves at low temperature of heating, suggesting that for these metals the crystal structure has a porous structure. These weakly bonded water molecules would be filling the structural available space. In porous hexacyanometallates the porous structure is usually related to vacancies for the building unit, in this case of the octahedral $[Fe(CN)_6]$ block. If the N end behaves as a single bridge and the metal linked to it has an octahedral coordination, 50% of the structural sites for the iron atom and of its six CN ligands will be vacant. Such a structure has enough free space to accommodate a large amount of weakly bonded water molecules. The coordination environment for the metal (T) located at the surface of a cavity generated by a vacancy of the building unit must be completed by coordinated water molecules because as average there are only three N ends available per metal. From these considerations, the metal coordination environment must be formed by three N ends plus three coordinated water molecules. For these two metals (Ni and Cu) the evolution of both weakly bonded and coordinated water molecules takes place as a continuous process. In porous cyanometallates the weakly bonded waters are stabilized within the cavities through hydrogen-bonding interactions with the coordinated ones [13,23]. Once the first hydrogen-bonded waters are removed, the remaining ones enhance their mutual interactions and a higher temperature to allow their release is required. This could explain the observed continuous weight loss for the TG curves. The weight loss detected for copper at 172 °C was attributed to liberation of a CN group, the first stage of its thermal decomposition process, an effect already observed for other copper hexacyanometallates [24]. For Ni a progressive weight loss from the dehydration stage until its decomposition is observed, without an intermediate temperature region of stability. In porous cyanometallates to Ni the smallest crystallite size corresponds [23–25]. This is attributed to a particularly strong interaction of the Ni atom with the CN groups generating local strains that limit the crystal growth process. The resulting small crystals, practically of colloidal nature, show a lower thermal stability due to their greater surface. In addition, the relatively high polarizing power for the Ni(2+) atom leads to a stronger interaction with its coordinated water molecules and a higher temperature for the water removal is required. These combined effects explain the observed features for the TG curve of the Ni complex salt.

For Co a more complex behavior on heating was observed, probably related to a more complex crystal structure. Below 55 °C the weakly bonded waters evolve, and then three stability regions are observed with two intermediate weight losses at 135 and 220 °C, attributed to liberation of coordinated water molecules (Fig. 1). This suggests the existence of two types of coordinated water molecules in the structure, evidence that is confirmed by IR spectroscopy and the refined crystal structure (discussed below). That behavior on heating does not correspond to a porous framework related to vacancies for the octahedral block, $[Fe(CN)_6]$, where the existence of only one type of coordinated water is possible.

3.2. IR spectra

The IR spectra of hexacyanometallates are composed of three vibrations within the octahedral unit, $M(CN)_6$: ν(CN), δ(MCN) and ν(MC); and those motions from crystal water, ν(OH) and δ(HOH), when it is present [26]. Fig. 2 shows the IR spectra for the studied series of hexacyanoferrates (II) and in Table 1 the frequency values for these vibrations are collected. For Zn the ν(CN) band is observed at 2108 cm^{-1}. This relatively high frequency for the ν(CN) band in a ferrocyanide suggests a tetrahedral coordination for the zinc atom. When the Zn atom is octahedrally coordinated to N ends of CN groups this vibration is observed below 2095 cm^{-1} [14]. Similar evidence is obtained from the frequencies for δ(FeCN) and ν(FeC) vibrations. For this compound a single and narrow δ(HOH) band at 1602 cm^{-1} is observed. This clearly indicates the existence of only one type of crystal water; the water molecule coordinated to the Zn atom. In the ν(OH) region two absorption bands at 3529 and 3596 cm^{-1} appear, ascribed to the symmetric and asymmetric OH stretching, respectively, of that coordinated water. Only a weak and broad absorption is detected below 3500 cm^{-1} where the ν(OH) absorption of hydrogen-bonded water must be observed. For Co, Ni and Cu the presence of a large amount of weakly bonded water molecules in the structure is evident from the broad ν(OH) bands below 3500 cm^{-1} and also by the bending δ(HOH) vibration around 1650 cm^{-1} (Fig. 2). The relatively high frequency for the ν(CN) band in the copper complex salt (2106 cm^{-1}) is attributed to a particularly strong interaction between the copper atom and the CN ligands. The ability of copper (2+) to received electrons in its $3d$ hole in order to adopt the $3d^{10}$ configuration is complemented by the CN group charge donation from its 5σ orbital, which has certain antibonding character, increasing the ν(CN) frequency [27]. A similar cooperative effect could also be contributing to the relatively high frequency observed for this vibration in the Ni complex salt.

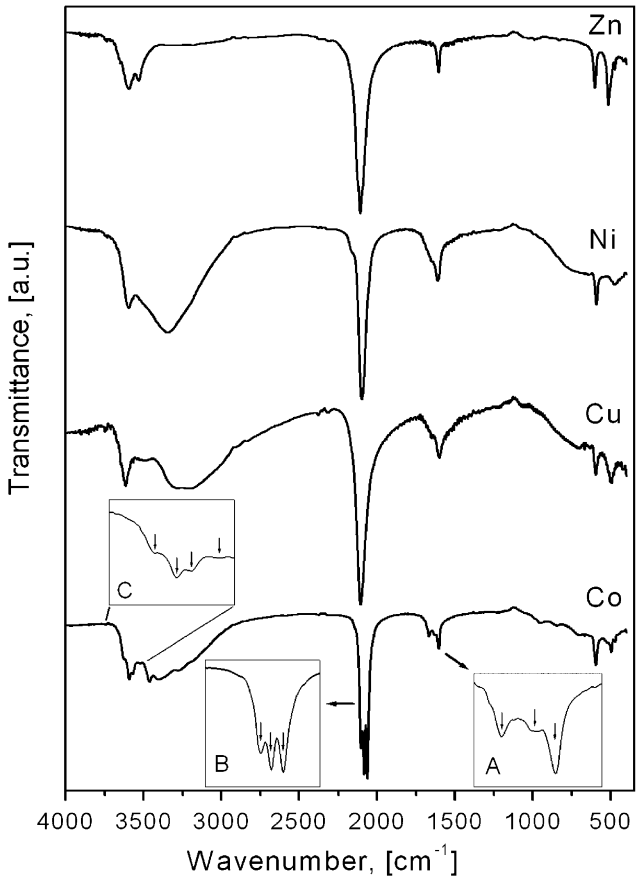

Fig. 2. IR spectra for the studied series of divalent transition metal hexacyanoferrates (II). In the Insets the fine structure in δ(HOH), ν(CN), and ν(OH) (for coordinated water molecules only) vibrations for Co is indicated.

Table 1
Frequency (in cm^{-1}) for the IR absorption bands observed in the studied compounds

Sample	ν(CN)	δ(FeCN)	ν(FeC)	$\nu(H_2O)_C$	$\nu(H_2O)_{HB}$	$\delta(H_2O)_C$	$\delta(H_2O)_{HB}$
$CO_2[Fe(CN)_6]\cdot 8.9H_2O$	2106, 2086, 2061	593	495	3629, 3594 3576, 3527	3466, 3405, 3273, 3186	1602, 1630	1670
$Ni_2[Fe(CN)_6]\cdot 10.5H_2O$	2098	591	476	3597, 3527	3352br	1607	1662sh
$Cu_2[Fe(CN)_6]\cdot 9.9H_2O$	2106	597	499	3621, 3506	3303, 3211	1602	1645
$Zn_2[Fe(CN)_6]\cdot 2.3H_2O$	2108	603	518	3529, 3596	–	1602	–

C: coordinated; HB: hydrogen bonded; br: broad; sh: shoulder.

For Co the IR spectrum provides valuable structural information. For this compound the ν(CN), ν(OH) and δ(HOH) vibrations show well-defined fine structures (see Fig. 2, insets). In the ν(CN) stretching region at least three bands at 2106, 2085 and 2061 cm^{-1} can be identified. The highest frequency band within the ν(CN) region corresponds to the IR forbidden A_{1g} symmetrical stretch, preceded by the also forbidden E_g degenerated unresolved doublet. The lower frequency band corresponds to the IR allowed F_{1u} degenerate stretch (an unresolved triplet) (Fig. 2, inset A). The appearance of the forbidden A_{1g} and E_g bands and their high intensity indicate that in this compound the building unit corresponds to a deformed octahedron. For the bending vibration of water at least three bands are well resolved (Fig. 2, inset B). The highest frequency band in the δ (HOH) vibrations region, at 1670 cm^{-1}, corresponds to the weakly bonded waters. The band at 1602 cm^{-1} is attributed to those water molecules with the stronger interaction with the metal, and the intermediate one at 1630 cm^{-1} also belongs to coordinated water molecules but with a weaker coordination bond. This assignment agrees with the above-discussed TG curve of this compound. In the ν(OH) vibrations region several bands are observed, four of them above 3500 cm^{-1}, corresponding to the two types of coordinated water molecules (Fig. 2, inset C). Below 3500 cm^{-1} the vibrations of the hydrogen-bonded waters are observed. The IR spectrum reveals that for Co the crystal structure is particularly complex and atypical.

3.3. Mössbauer spectra

The Mössbauer spectrum senses the valence, electronic configuration, and symmetry of the charge environment for the iron atom. Figs. 3(a–d) show the Mössbauer spectra recorded for the studied series of hexacyanoferrates (II). According to the estimated isomer shift values (Table 2) the iron atom is found with a low-spin electronic configuration, an expected result, due to the bonding properties of the CN ligand. These spectra are single lines corresponding to a symmetrical charge environment for the iron atom. To the value of Δ for low spin Fe(II) in hexacyanoferrates only the environment of ligands contributes (lattice contribution to Δ). Even for Co where IR spectrum detects certain deformation for the octahedral building block, the Mössbauer spectrum is a single line but with a slight broadening.

3.4. Crystal structures

The crystal structures were solved considering the above-discussed structural information from TG, IR, and Mössbauer data and also using physical considerations regarding acceptable variation limits for the Fe–C and C–N interatomic distances and C–Fe–C and Fe–C–N bond angles. Due to the nature of the bonding structure, for the Fe–C–N chain no large deviations from the linearity are expected. The iron atom receives charge through its e_g orbitals from the CN group. This σ bonding interaction induces certain π-back donation from the metal t_{2g} orbitals to the ligand

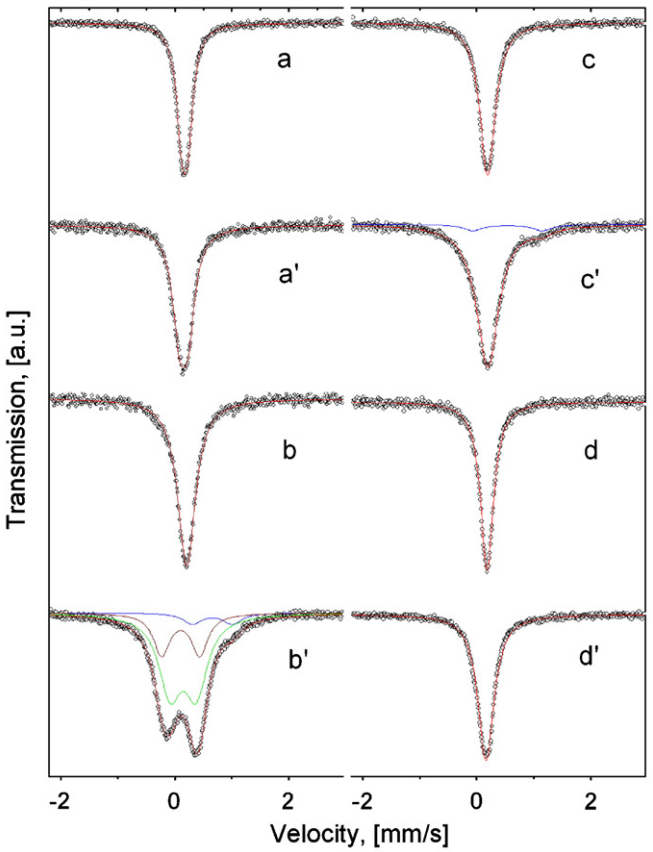

Fig. 3. Mössbauer spectra at room temperature for the studied series of hexacyanoferrates (II). a (Co), b (Ni), c (Cu), d (Zn): spectra for the as-synthesized samples; a′ (Co), b′(Ni), c′(Cu), d′(Zn): spectra for the samples heated for 2 h at the dehydration temperature and then rehydrated in air for two days. Enlarged versions of these spectra are available from Supplementary Information.

Table 2
Mössbauer parameters at room temperature for the studied compounds before and after their heating at the dehydration temperature indicated by the TG curve

Sample	δ[a] (mm/s)	Δ (mm/s)	Γ (mm/s)	A (%)	Assignment
CO_2Fe before heating	0.16	0.09	0.25	100	LS Fe(II)
CO_2Fe heated at 230 °C	0.16	0.14	0.30	100	LS Fe(II)
Ni_2Fe before heating	0.19	–	0.40	100	LS Fe(II)
Ni_2Fe heated at 150 °C	0.14	0.46	0.41	66	LS Fe(II)
	0.10	0.67	0.35	26	LS Fe(II)
	0.65	0.70	0.39	8	HS Fe(3+)
Cu_2Fe before heating	0.17	–	0.33	100	LS Fe(II)
Cu_2Fe heated at 70 °C	0.17	–	0.36	95	LS Fe(II)
	0.54	1.22	0.41	5	HS Fe(3+)
Zn_2Fe before heating	0.17	–	0.28	100	LS Fe(II)
Zn_2Fe heated at 200 °C	0.17	–	0.34	100	LS Fe(II)

Fitting error in δ, Δ and Γ remains below 0.01 mm/s. LS: low spin; HS: high spin.
[a] The value of δ is reported relative to sodium nitroprusside.

anti-bonding orbitals at the C end. The net effect is the formation of a strong Fe–CN bond with participation of three orbitals from the iron atom, which shows a relatively high rigidity. C and N atoms are also involved in triple-bonding interaction with also certain rigidity. A higher flexibility and deviation from the linearity for the N–*T*–N angle are possible due to the nature of the involved bonding interaction. For the rhombohedral phase of Zn hexacyanometallates, for instance, where the Zn atom is tetrahedrally coordinated to N ends, the N–Zn–N angle is close to 108° [14].

For Zn, from the pattern indexing, using the DICVOL code [19], a hexagonal unit cell with $a = b = 7.59$, $c = 5.74$ Å was found with figures of merit $M(21) = 103$ and $F(21) = 87$. The estimated unit cell volume (285.88 Å^3) corresponds to a relatively compact structure with $Z = 1$ (a formula unit per cell). From the extinction analysis the possible space groups were reduced to eight groups (*P*3, *P*312, *P*321, *P*3*m*1, *P*31*m*, *P*-3, *P*-31*m*, *P*-3*m*1). Considering the multiplicity of these groups the structure was solved in parallel for the three center symmetric ones (*P*-3, *P*-31*m*, *P*-3*m*1) using direct methods. Only for *P*-3 (147) a structure according to the information derived from TG and IR data and the mentioned physical considerations were obtained. In this structure the Zn atom is found coordinated to three N ends plus a water molecule to form a deformed tetrahedron (see Supplementary Information) related to the different bonding properties for the CN group and the water molecule. Fig. 4 shows the experimental and fitted XRD patterns and their difference. Details on the refinement parameters, the refined atomic positions, bond distances and angles, and thermal and occupation factors are available from the Supplementary Information. Fig. 5 shows the atomic packing within the unit cell and the coordination environments for the metal centers. The porous network of this compound is formed by a system of narrow and interconnected channels (Fig. 6). Crystal structures based on *P*-3 (147) space group have also been found for other hexacyanometallates, with an atypical coordination environment for the metal linked at the N end of the CN group and also a 2:1 metals ratio in the formula unit [17].

For Ni and Cu the recorded XRD patterns are quite similar (Fig. 7), suggesting that these two compounds crystallize with analogous unit cells. From the index assignment a cubic cell with cell edge close to 10 Å was obtained. The estimated reliability indexes (merit figures) for this assignment were relativity high, $M(18) > 77$ and $F(18) > 54$. Such a cell edge value is typical for cubic hexacyanometallates and corresponds to the

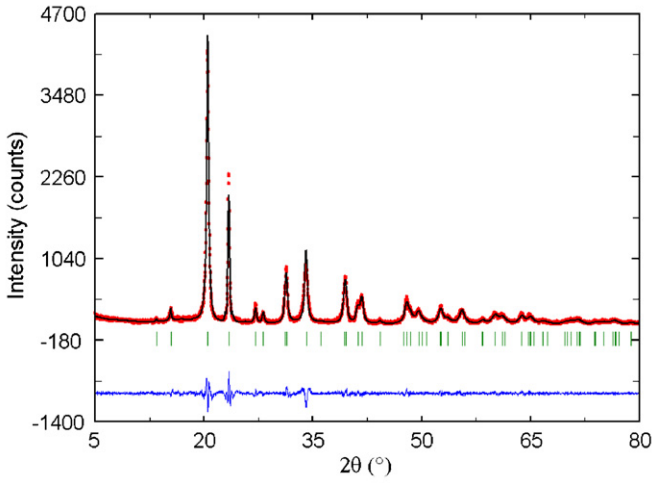

Fig. 4. XRD powder pattern observed (red), calculated (black) and difference profile (blue) for the Rietveld refinement of $Zn_2[Fe(CN)_6] \cdot 2.3H_2O$.

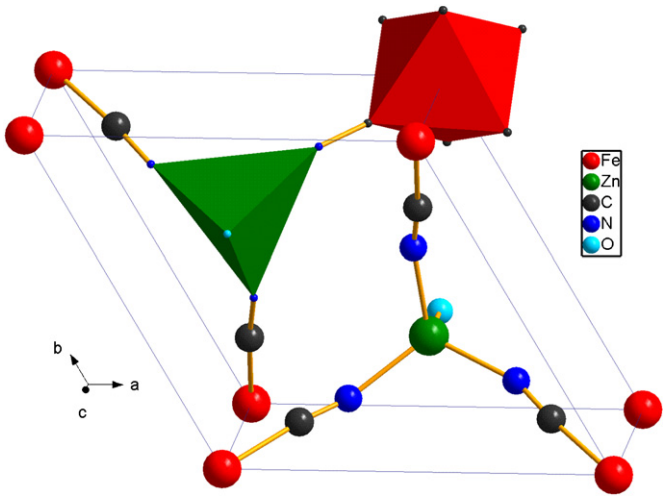

Fig. 5. Atomic packing within the unit cell for $Zn_2[Fe(CN)_6] \cdot 2H_2O$. The Zn atom has a tetrahedral coordination to three N ends plus a water molecule.

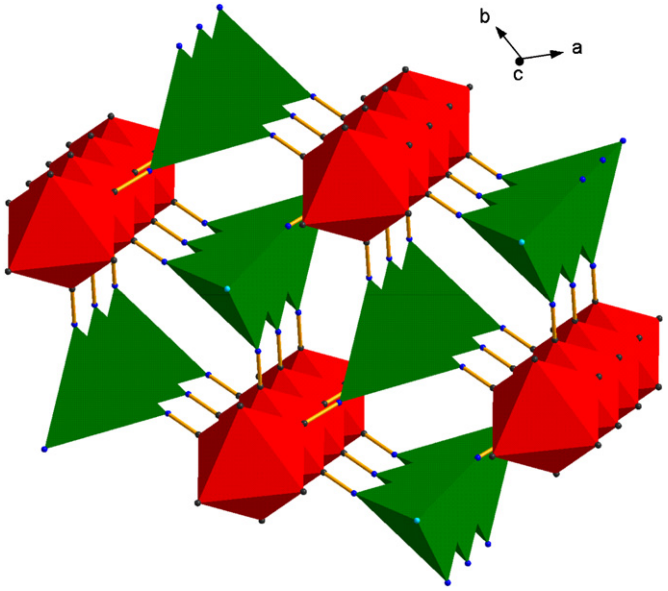

Fig. 6. Porous framework of $Zn_2[Fe(CN)_6] \cdot 2H_2O$. Related to tetrahedral coordination for Zn, a system of narrow channels is formed.

T–N–C–M–C–N–*T* chain length [13]. From the extinction analysis, the possible space groups were reduced to five: *P*23, *P*432, *P*-43*m*, *Pm*-3, and *Pm*-3*m*. The structure resolution for the group of highest symmetry, *Pm*-3*m* (221), produced an appropriate structural model, compatible with the "*a priori*" available information for these two compounds. This model was then refined in order to obtain the atomic positions, and thermal and occupation factors, and to estimate the bond distances and angles. Details on the refinement process and the values obtained for all these parameters are available from the Supplementary Information. The estimated bond distances and angles are within the expected values for cubic hexacyanoferrates (II) [13,28]. The hydration degree, estimated from the occupation factors for the oxygen atom of water molecules (coordinated plus hydrogen bonded), is similar to that derived from the TG curves. Fig. 8 shows the atomic packing within the unit cell and the coordination environment for the metal centers. The coordination sphere for the metal (Ni, Cu) is formed by three N ends of CN group plus

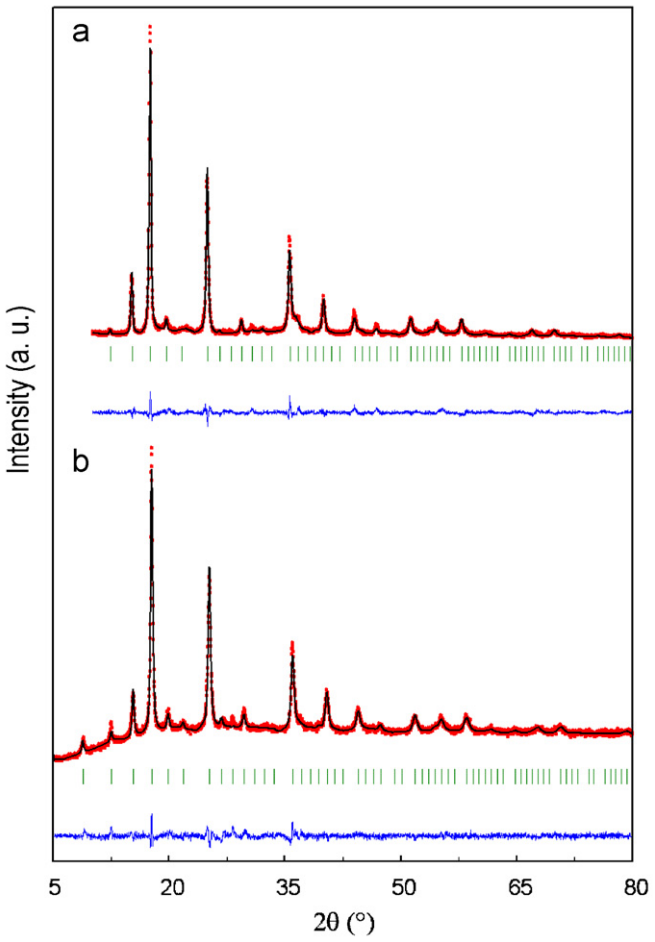

Fig. 7. XRD powder patterns observed (red), calculated (black), and difference profile (blue) for the Rietveld refinement of $T_2[Fe(CN)_6]\cdot xH_2O$ with T = Ni (a) and Cu (b).

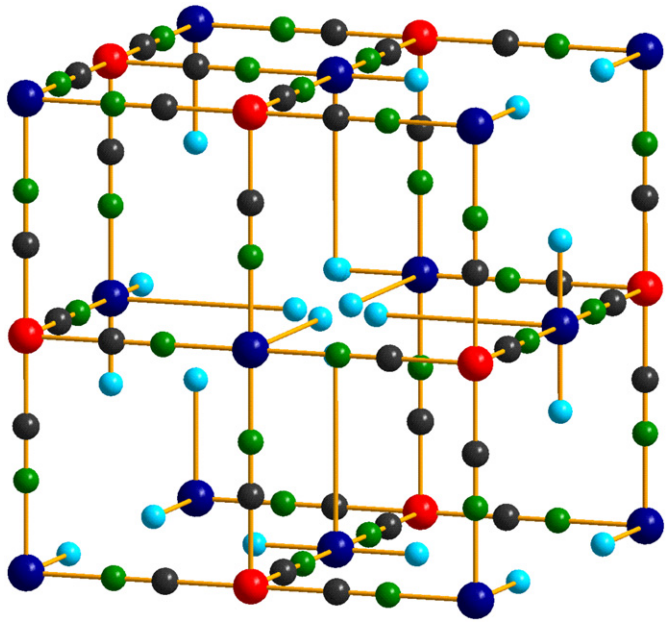

Fig. 8. Atomic packing and metals coordination environments in $T_2[Fe(CN)_6]\cdot xH_2O$ with T = Ni, Cu. The hydrogen-bonded water molecules have been omitted. The Ni (Cu) atom is coordinated to three N ends plus three water molecules.

three water molecules. The occupation of the free volume within the framework is completed by water molecules hydrogen bonded to the coordinated ones. Due to the large amount of vacant sites for the octahedral unit (50%), the resulting cavities remain interconnected to form a system of channels. The cell volume per formula unit is 508.76 Å^3 for Ni and 494.45 Å^3 for Cu, close to 2 times the value found for Zn (285.88 Å^3). The relatively smaller value of this parameter for Cu is related to the above-discussed strong interaction of the copper atom with the CN group, where the unit cell edge results 9.9628(5) Å. The large values for the cell volume per formula unit for Cu and Ni indicate that their structure is relatively open, where a large free volume is available.

For Co the XRD powder pattern (Fig. 9) corresponds to a unit cell of low symmetry (monoclinic). From the extinction analysis two space groups were found to be possible: $P2/m$ and $P2_1/m$. The unit cell parameters, estimated from the Le Bail profile fitting, are $a = 7.406$, $b = 9.368$, $c = 11.700$ Å, with $\beta = 92.36^\circ$. According to the volume of this cell, 816.44 Å^3, and considering $Z = 2$, a volume per formula unit of 408.22 Å^3 results, close to the value found for the cubic cell (Ni and Cu). This suggests that a large volume fraction of the unit cell for Co could be occupied by water molecules. The model to be refined was derived for $P2_1/m$ (11) space group using Patterson electron density maps calculated using the program SHELXS from extracted intensities according to the Le Bail method [21]. Due to the low symmetry of the unit cell for Co, the number of parameters to be refined is extremely high (77). Details on the refinement process and the refined values for the atomic positions, thermal and occupation factors, and the estimated bond distances and angles are available from the Supplementary Information. Fig. 10 shows the atomic packing within the unit cell and the coordination environment for the metal centers. The $P2_1/m$ structural model has two sites for the Co atom. In one of these sites cobalt was found tetrahedrally coordinated to N ends of CN groups, and the other site the coordination environment is formed by two CN groups plus four water molecules. The coordination bond is stronger for the axial waters and weaker for the equatorial ones where also the two CN groups are found (see Supplementary Information). This explains the above-discussed evidence from TG and IR data on the existence of two types of coordinated water molecules. This compound adopts a structure of stacked layers. Neighboring layers remain linked through a network of hydrogen-bonding interactions between the coordinated and weakly bonded waters (Fig. 11). Practically all the crystal water is found in the region

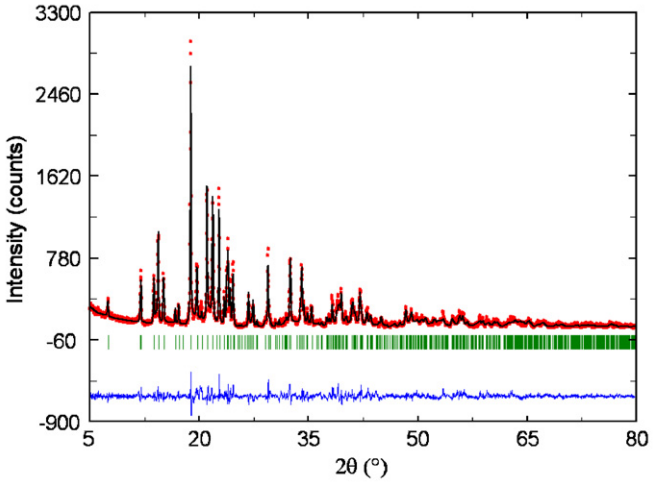

Fig. 9. XRD powder patterns observed (red), calculated (black), and difference profile (blue) for the Rietveld refinement of $Co_2[Fe(CN)_6]\cdot xH_2O$.

between layers. When these weakly bonded waters are removed by heating below 55 °C (Fig. 1), the layers remain together through van der Walls interactions. Structure of layers has also been reported for copper transition metal pentacyanonitrosylferrate (II) [29].

In Table 3 the estimated cell parameters, cell volume per formula unit, and space group for all the studied compositions are summarized. The crystal structures found for this series of divalent transition metals hexacyanoferrates (II) are quite different to that already reported for Mn and Cd analogues where neighboring metal centers remain linked by two aquo bridges [15,16]. Regarding magnetic properties, for Co, Ni, and Cu, a weak antiferromagnetic ordering is expected corresponding to identical atoms (*T*) with their electron clouds coupled through the *T*–N–C–Fe–C–N–*T* chain, similar to the already reported behavior for Zn hexacyanoferrate (III) [14].

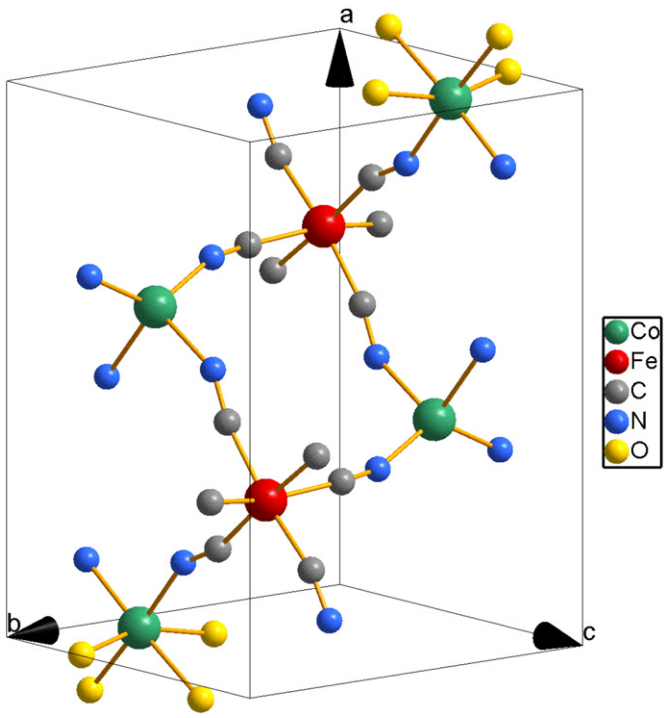

Fig. 10. Atomic packing within the unit cell and coordination environment for Fe and CO atoms in $Co_2[Fe(CN)_6]\cdot xH_2O$. The structure contains two positions for the Co atom.

3.5. *Framework stability on the water removal and H_2 storage*

Figs. 3(a′–d′) show the Mössbauer spectra for samples heated for 3 h at the dehydration temperature indicated by the TG curves (Co:230, Ni:150, Cu:70, Zn:200 °C) and then rehydrated at air for two days. An enlarged version of these spectra is available from the Supplementary Information. For Co the spectrum can be fitted as an unresolved doublet. This suggests that the heating and the related water molecules removal induce certain structural disorder but not sample decomposition. The isomer shift value of this doublet (Table 2) is similar to that found for the initial (non-heated) sample where the iron atom is coordinated to six C ends of CN groups. For Ni the spectrum of the heated sample can be fitted as three quadrupole doublets. The two most intense doublets correspond to low spin Fe(II), according to their isomer

Table 3
Unit cell parameters, cell volume per formula unit and space group for the studied compounds

Compound	Unit cell parameters (Å)	Cell volume per formula unit	Space group
$CO_2[Fe(CN)_6]\cdot 8.9H_2O$	$a = 11.7242(9)$ $b = 9.3959(6)$ $c = 7.4191(3)$ $\beta = 92.6224°(9)$	408.22(3)	$P2_1/m$ (11)
$Ni_2[Fe(CN)_6]\cdot 10.5H_2O$	10.0646(8)	508.76(2)	Pm-3m (221)
$Cu_2[Fe(CN)_6]\cdot 9.9H_2O$	9.9628(5)	494.45(2)	Pm-3m (221)
$Zn_2[Fe(CN)_6]\cdot 2.3H_2O$	$a = b = 7.5843(8)$ $c = 5.7387(1)$ $\gamma = 120°$	285.88(1)	P-3 (147)

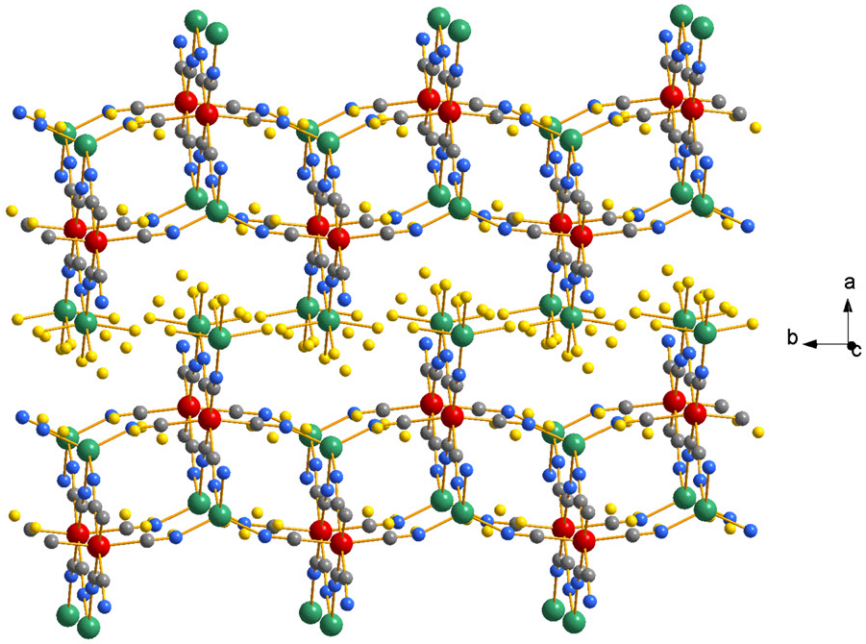

Fig. 11. Structure of stacked layers for $Co_2[Fe(CN)_6]\cdot xH_2O$. These layers remain linked through a network of hydrogen-bonding interactions between coordinated and weakly bonded water molecules.

shift values. This indicates that the iron atom remains coordinated to the C end of six CN groups. The large quadrupole splitting values observed for these two doublets are sensing certain structural disorder related to the crystal water removal. The observed variation for the values of δ relatively to the non-heated sample was attributed to that structural disorder. The isomer shift value estimated for the weaker doublet is characteristic of high spin Fe(3+), ascribed to a decomposition by-product. An analogous doublet has been reported for partially decomposed hexacyanoferrates [24]. The behavior observed for Cu is similar to that already mentioned for Co but with the appearance of a small fraction of high-spin Fe(3+), indicating that partial sample decomposition has taken place. Even a relatively low temperature of heating (70 °C) is sufficient to induce decomposition in the copper complex salt. For Zn the TG curve suggested that the anhydrous phase shows a relatively high stability, at least compared with the remaining compositions (Co, Ni, Cu) (Fig. 1). Analogue evidence is obtained from the Mössbauer spectrum. Only a slight peak broadening was observed for the rehydrated Zn sample (Fig. 3d′, Table 2).

As already mentioned, the hydrogen storage in anhydrous hexacyanoferrates (II) with supposedly 50% of vacancy for the building unit has been reported [9]. Such a large amount of vacancies leads to a high free volume with 50% of the metal coordination sites available for interaction with the hydrogen molecule. From these considerations, H_2 adsorption isotherms for different dehydration temperatures and heating times were recorded. Considering that under vacuum a lower temperature to obtain anhydrous samples is required, sample dehydration temperatures below those suggested by the TG curves were also considered. Without exception, for Ni and Cu always evidence of collapse for the porous framework was obtained. Fig. 12 shows a typical set of H_2 isotherms. For Co the structure of layers was found to be inaccessible to the H_2 molecule. Only for Cu, the compound that becomes anhydrous at the lowest temperature of heating, an appreciable H_2 adsorption was observed, but the maximum adsorption is significantly smaller than that found for copper hexacyanocobaltate (III) with only 33.33% of vacancies (Fig. 12). For Zn no H_2 adsorption was observed. This behavior for Zn is consistent with previous studies for the H_2 adsorption in materials with narrow channels [30]. The porous framework accessibility and stability for this series of hexacyanoferrates (II) was also studied from CO_2 adsorption data (see Supplementary Information). The results were similar to those obtained from H_2 adsorption. On the water removal the porous framework for Ni and Cu, with 50% of vacancies, collapses.

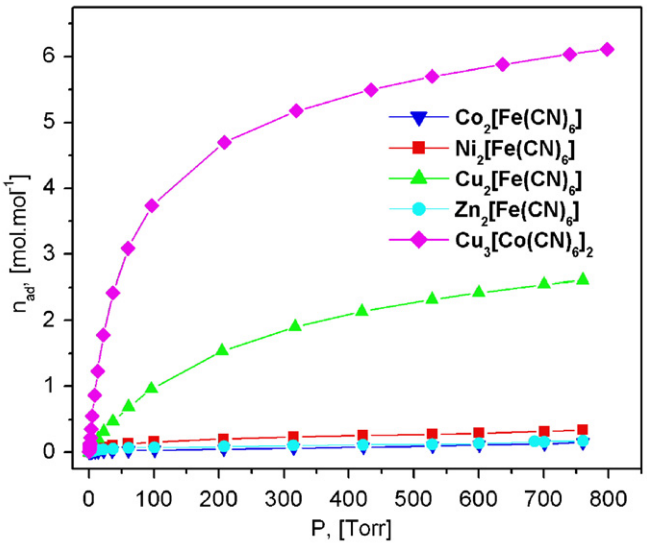

Fig. 12. H_2 adsorption isotherms for the studied series of hexacyanoferrates (II). For comparison, the H_2 isotherm in $Cu_3[CO(CN)_6]_2$ with only 33% of vacancies for the building block is included.

4. Conclusions

The crystal structures for $T_2[Fe(CN)_6]\cdot xH_2O$ with T = Co, Ni, Cu and Zn were solved and refined. For Ni and Cu the metal linked at the N end of the CN group appears with an octahedral coordination sphere formed by three N atoms plus three water molecules. In their structure 50% of the structural sites for the building block, $[Fe(CN)_6]$, remain vacant, generating an open channel framework. The cavities generated by the vacancies remain filled with coordinated and hydrogen-bonded waters. When these water molecules are removed, the porous framework collapses. For Co a structure of stacked layers was obtained with the cobalt atom in both tetrahedral and octahedral coordination. In the as-synthesized materials neighboring layers remain linked through hydrogen-bonding interactions between coordinated and weakly bonded water molecules. For Zn, a porous structure formed by narrow channels was observed related to a tetrahedral coordination for the Zn atom. That free volume was found to be inaccessible to H_2. The zinc atom coordination sphere is formed by three N ends of CN group plus a coordinated water molecules. The solved and refined crystal structures are supported by the TG, IR and Mössbauer data. The structures and related properties for this series of divalent transition metal hexacyanoferrates (II) have not been previously reported.

Supplementary information

Structural information derived from the crystal structures refinement has also been deposited at ICSD Fachinformationszentrum Karlsruhe (FIZ) (E-mail: crysdatafiz-karlsruhe.de) with CSD file numbers: 419452:$CO_2[Fe(CN)_6]\cdot xH_2O$; 419453:$Ni_2[Fe(CN)_6]\cdot xH_2O$; 419454:$Cu_2[Fe(CN)_6]\cdot xH_2O$; 419455:$Zn_2[Fe(CN)_6]\cdot 2.3H_2O$. Additional supplementary information is available free of charge via the Internet at doi:10.1016/j.jssc.2008.07.030.

Acknowledgments

L.R. acknowledges the support provided by the ALFA Project NANOGASTOR for her PhD studies. The help of C.P. Krap for the H_2 adsorption data collection is highly appreciated. This research was partially supported by the Projects SEP-2004-C01-47070 and SEP-CONACyT-2007-61541. The authors thank E. Fregoso-Israel from IIM-UNAM for the TG data collection.

Appendix A. Supplementary information

The online version of this article contains additional supplementary data. Please visit doi:10.1016/j.jssc.2008.07.030

References

[1] S. Ferlay, T. Mallah, R. Ouahes, P. Veillet, M. Verdaguer, Nature 378 (1995) 701.
[2] O. Sato, T. Iyoda, A. Fujishima, K. Hashimoto, Science 272 (1996) 704.
[3] V. Escax, A. Bleuzen, J. Itié, P. Munsch, F. Varret, M. Verdaguer, J. Phys. Chem. B 107 (2003) 4763.
[4] S. Ohkoshi, K. Arai, Y. Sato, K. Hashimoto, Nat. Mater. 3 (2004) 857.

[5] R. Martínez-García, M. Knobel, E. Reguera, J. Phys.: Condens. Matter 18 (2007) 11243.
[6] S.S. Kaye, J.R. Long, J. Am. Chem. Soc. 127 (2005) 6506.
[7] K.W. Chapman, P.D. Southon, C.L. Weeks, C.J. Kepert, Chem. Commun. (2005) 3322.
[8] M.R. Hartman, V.K. Peterson, Y. Liu, S.S. Kaye, J.R. Long, Mater. Chem. 18 (2006) 3221.
[9] S.S. Kaye, J.R. Long, Catal. Today 120 (2007) 311.
[10] S.S. Kaye, J.R. Long, Chem. Commun. (2007) 4486.
[11] L. Reguera, J. Balmaseda, L.F. del Castillo, E. Reguera, J. Phys. Chem. C 112 (2008) 5589.
[12] L. Reguera, J. Balmaseda, M. Avila, E. Reguera, J. Phys. Chem. C 112 (2008) Accepted.
[13] A. Ludi, A. Gudel, Struct. Bonding 14 (1973) 1.
[14] J. Rodríguez-Hernandez, E. Reguera, E. Lima, J. Balmaseda, R. Martinez-Garcia, H. Yee-Madeira, J. Phys. Chem. Solid 68 (2007) 1630 and references therein.
[15] M. Rueg, A. Ludi, K. Rieder, Inorg. Chem. 10 (1971) 1775.
[16] A. Gómez, E. Reguera, Int. J. Inorg. Mater 3 (2001) 1045.
[17] J. Rodríguez-Hernandez, A. Gomez, E. Reguera, J. Phys. D: Appl. Phys. 40 (2007) 6076 and reference therein.
[18] G. Brauer, Handbook of Preparative Inorganic Chemistry, vol. 2, 2nd ed., Academic Press, New York, 1965, p. 1373.
[19] D. Louer, R. Vargas, J. Appl. Crystallogr. 15 (1982) 542.
[20] G.M. Sheldrick, Program for Crystal Structure Determination, Institute fur Anorg. Chemie, Göttingen, Germany, 1997.
[21] A.L. Le Bail, ESPOIR: A Program for Solving Structures by Monte Carlo from Powder Diffraction Data, in EPDIC-7. Barcelona, 2000, 〈http://www.cristal.org/sdpd/espoir/〉.
[22] J. Rodríguez-Carvajal, The FullProf Program, Institute Louis Brilloin, Saclay, France, 2005.
[23] J. Roque, E. Reguera, J. Balmaseda, J. Rodriguez-Hernandez, L. Reguera, L.F. del Castillo, Micropor. Mesopor. Mater 103 (2007) 57.
[24] R. Martinez-Garcia, M. Knobel, E. Reguera, J. Phys. Chem. B 110 (2006) 7296.
[25] A. Gomez, J. Rodríguez-Hernandez, E. Reguera, Powder Diffr. 22 (2007) 27.
[26] K. Nakamoto, Infrared and Raman Spectra of Inorganic and Coordination Compounds, Wiley, New York, 1986, p. 484.
[27] E. Reguera, J. Rodríguez-Hernandez, A. Champi, J.G. Duque, E. Granado, G. Rettori, Z. Phys. Chem. 220 (2006) 1609.
[28] F. Herren, P. Fischer, A. Ludi, W. Halg, Inorg. Chem. 19 (1980) 956.
[29] A. Gómez, J. Rodriguez-Hernandez, E. Reguera, J. Chem. Crystallogr. 34 (2004) 893.
[30] L. Reguera, J. Balmaseda, C.P. Krap, E. Reguera, J. Phys. Chem. C 112 (2008) 10490.